An Exponential Family of Hyperbolic–Type Controllers[1]

FRANCISCO TERNEUS [I,II], FERNANDO REYES[III] and EDUARDO LEBANO[II].
[II]Centro Interdisciplinario de Posgrados, Maestría en Mecatrónica
[III]Grupo de Robótica, Facultad de Ciencias de la Electrónica
[I] Escuela Superior Politécnica del Ejercito, Quito, Ecuador
[II]Universidad Popular Autónoma del Estado de Puebla
[III]Benemérita Universidad Autónoma de Puebla
Apartado Postal 542, Puebla 72001, México
Tel/Fax: +(52) 222 2 29 55 00 ext. 7410
MÉXICO
e-mail: freyes@ece.buap.mx; pacoterneus@hotmail.com

Abstract: This paper addresses the problem of position control for robot manipulators. An Exponential family of Hyperbolic–Type controllers for robot manipulators is presented. The proposed family consists of a large class of control algorithms with nonlinear structure, which incorporates components of hyperbolic type to quickly drive the position error to zero position. We provide explicit sufficient conditions for ensuring directly global asymptotic stability of the closed-loop system composed by the nonlinear robot dynamics for n degrees of freedom and the proposed scheme. Besides the theoretical results, a real-time experimental comparison is also presented to illustrate the performance of the proposed family with other well-known control algorithms such as PD and Hyperbolic Tangent schemes on a three degrees of freedom direct-drive robot arm.

Key-Words: Global asymptotic stability, Lyapunov function, PD controller, robot manipulators, position control.

1 Introduction

Today, robot manipulators offer interesting theoretical and practical challenges of control researchers due to the non-linear and multivariable nature of their dynamical behavior [1] [2] [3] . In particular, the position control or also so-called regulation problem of rigid robots has attracted a considerable amount of attention (see [4] and the references cited therein). It may be recognized as the simplest aim in robot control and it is one of the most relevant issues in the practice of manipulators. The regulation problem consists in moving the manipulator from any initial state to a fixed desired configuration.[5] [6] The problem of designing regulators is ensuring asymptotic position error and joint velocity to zero. Regulators that achieve this objective for all desired targets and all initial conditions are said to be globally convergent.[7]

Lyapunov functions are an indispensable tool in analysis and design of controllers for nonlinear systems and play an important role in the stability study of robot manipulators. The asymptotic stability is achieved using the LaSalle invariance principle[9] . We use the methodology by energy shaping plus damping injection technique introduced by Takegaki and Arimoto[10] to study the simple PD control with gravity compensation, which can be considered as a landmark in robot control. Using energy shaping it yields a global stable closed–loop system for a trivial selection of proportional and derivative gains, and applying the LaSalle's invariance principle the asymptotic stability is achieved.[11] . Many authors have used energy shaping to design control schemes using a weak Lyapunov function [41] [39] [40].They obtain a global stable closed–loop system. The global asymptotic stability is obtained with the LaSalle's invariance principle.[13] [14] [15] [16] [17] [18]

In view of the simplicity and applicability of the

[1]Work partially supported by CONACYT 91503, México

simple PD controller in industrial applications, the purpose of this paper is to unify the previous results of the linear PD control on a large class of Hyperbolic-type controllers for robot manipulators that lead to global asymptotic stability of the closed–loop system (dynamics model of robot manipulator plus controller) using the direct method of Laypunov. The proposed control scheme has a nonlinear structure, which incorporates components of hyperbolic type to quickly drive the position error to zero position. In addition to the theoretical issues of the proposed family; this paper also presents a real-time comparative study of five position controllers : three membership controllers of the proposed family vs. Hyperbolic Tangent and PD controllers on a three degrees of freedom direct–drive arm.

This paper is organized as follows. Section 2 recalls the robot dynamics and useful properties for stability proof. In Section 3, the proposed hyperbolic family is presented and its analysis of global asymptotic stability with a Lyapunov function is also proposed. Section 4 summarizes the main components of the experimental set–up. Section 5 contains the experimental comparison with three controllers of proposed family vs PD and Hyperbolic Tangent controllers on a three degrees of freedom arm. Finally, some conclusions are offered in Section 6.

2 Robot Dynamics

In the absence of friction phenomena and other disturbances, the dynamics of a serial n-link rigid robot can be written as:[31]

$$M(\boldsymbol{q})\ddot{\boldsymbol{q}} + C(\boldsymbol{q},\dot{\boldsymbol{q}})\dot{\boldsymbol{q}} + \boldsymbol{g}(\boldsymbol{q}) = \boldsymbol{\tau} \qquad (1)$$

where $\boldsymbol{q}$ is the $n \times 1$ vector of joint displacements, $\dot{\boldsymbol{q}}$ is the $n \times 1$ vector of joint velocities, $\boldsymbol{\tau}$ is the $n \times 1$ vector of input torques, $M(\boldsymbol{q})$ is the $n \times n$ symmetric positive definite manipulator inertia matrix, $C(\boldsymbol{q},\dot{\boldsymbol{q}})$ is the $n \times n$ matrix of centripetal and Coriolis torques, and $\boldsymbol{g}(\boldsymbol{q})$ is the $n \times 1$ vector of gravitational torques obtained as the gradient of the robot potential energy due to gravity.

It is assumed that the robot links are joined together with revolute joints. Although the equation of motion (1) is complex, it has several fundamental properties which can be exploited to facilitate control system design. For the proposed controller, the following important properties are used:

Property 1. The inertia matrix $M(\boldsymbol{q})$ is symmetric, positive definite, therefore $\exists\, M(\boldsymbol{q})^{-1}$ and it is also a symmetric, positive definite matrix. Both $M(\boldsymbol{q})$ and $M(\boldsymbol{q})^{-1}$ are uniformly bounded as a function of $\boldsymbol{q} \in \mathbb{R}^n$, this is $||M(\boldsymbol{q})|| < \beta$, where β is a positive real constant, strictly speaking, boundedness of the inertia matrix requires in general, that all joints be revolute:[19] [33]

$$\beta \;\geq\; n\left(\max_{i,j,\boldsymbol{q}} |M_{ij}(\boldsymbol{q})|\right)$$

where M_{ij} are elements of $M(\boldsymbol{q})$.

Property 2. See Koditschek[19] Spong & Vidyasagar[31] and Romeo *et al.* [33] the matrix $C(\boldsymbol{q},\dot{\boldsymbol{q}})$ defined using the Christoffel symbols and the time derivative $\dot{M}(\boldsymbol{q})$ of the inertia matrix satisfy:

1. $\dot{\boldsymbol{q}}^T\left[\frac{1}{2}\dot{M}(\boldsymbol{q}) - C(\boldsymbol{q},\dot{\boldsymbol{q}})\right]\dot{\boldsymbol{q}} = \boldsymbol{0} \;\; \forall\, \boldsymbol{q},\dot{\boldsymbol{q}} \in \mathbb{R}^n.$
2. $\dot{M}(\boldsymbol{q}) = C(\boldsymbol{q},\dot{\boldsymbol{q}}) + C(\boldsymbol{q},\dot{\boldsymbol{q}})^T \;\; \forall\, \boldsymbol{q},\dot{\boldsymbol{q}} \in \mathbb{R}^n.$

Property 3. The Coriolis matrix $C(\boldsymbol{q},\dot{\boldsymbol{q}})$satisfies the following:[31] [33]

1. If $\dot{\boldsymbol{q}} = \boldsymbol{0}$ then $C(\boldsymbol{q},\dot{\boldsymbol{q}}) = 0 \in \mathbb{R}^{n\times n} \quad \forall \boldsymbol{q} \in \mathbb{R}^n$.
2. $\dot{\boldsymbol{q}}^T C(\boldsymbol{q},\dot{\boldsymbol{q}})\dot{\boldsymbol{q}}$ is bounded as a function of $\boldsymbol{q},\dot{\boldsymbol{q}} \in \mathbb{R}^n$, then $||\dot{\boldsymbol{q}}^T C(\boldsymbol{q},\dot{\boldsymbol{q}})\dot{\boldsymbol{q}}|| < ||\boldsymbol{q}||^2 k_c$, where $k_c \in \mathbb{R}_+$.

3 An Exponential Hyperbolic Family –Type Controllers

This section presents the proposed exponencial hyperbolic family of controllers and its global asymptotic stability analysis. We intend to extend the results on the simple PD controller to a large class of hyperbolic-type controllers for robot manipulators. Consider the following control scheme with gravity compensation given by

$$\begin{aligned}\boldsymbol{\tau} &= K_p \frac{ch(\lambda\tilde{\boldsymbol{q}})^{m-1} sh(\lambda\tilde{\boldsymbol{q}})}{1 + ch(\lambda\tilde{\boldsymbol{q}})^m} \\ &- K_v \frac{ch(\alpha\dot{\boldsymbol{q}})^{m-1} sh(\alpha\dot{\boldsymbol{q}})}{1 + ch(\alpha\dot{\boldsymbol{q}})^m} + \boldsymbol{g}(\boldsymbol{q}) \qquad (2)\end{aligned}$$

where $K_p \in \mathbb{R}^{n\times n}$ is the proportional gain which is a diagonal matrix, $K_v \in \mathbb{R}^{n\times n}$ is a positive

definite matrix, so-called derivative gain, and the following terms are defined as:

$$\frac{ch(\lambda\tilde{\boldsymbol{q}})^{m-1}sh(\lambda\tilde{\boldsymbol{q}})}{1+ch(\lambda\tilde{\boldsymbol{q}})^{m}} = \begin{bmatrix} \frac{ch(\lambda_1\tilde{q_1})^{m-1}sh(\lambda_1\tilde{q_1})}{1+ch(\lambda_1\tilde{q_1})^{m}} \\ \vdots \\ \frac{ch(\lambda_n\tilde{q_n})^{m-1}sh(\lambda_n\tilde{q_n})}{1+ch(\lambda_n\tilde{q_n})^{m}} \end{bmatrix} \quad (3)$$

$$\frac{ch(\alpha\dot{\boldsymbol{q}})^{m-1}sh(\alpha\dot{\boldsymbol{q}})}{1+ch(\alpha\dot{\boldsymbol{q}})^{m}} = \begin{bmatrix} \frac{ch(\alpha_1\dot{q_1})^{m-1}sh(\alpha_1\dot{q_1})}{1+ch(\alpha_1\dot{q_1})^{m}} \\ \vdots \\ \frac{ch(\alpha_n\dot{q_n})^{m-1}sh(\alpha_n\dot{q_n})}{1+ch(\alpha_n\dot{q_n})^{m}} \end{bmatrix} \quad (4)$$

where λ_i and $\alpha_i \in \mathbb{R}_+$, m is the exponent, which is a positive integer number, $\tilde{\boldsymbol{q}} \in \mathbb{R}^n$ is the position error vector, which is defined as $\tilde{\boldsymbol{q}} = \boldsymbol{q}_d - \boldsymbol{q}$, with $\boldsymbol{q}_d \in \mathbb{R}^n$ represents the desired joint position; ch() and sh() are the hyperbolic cosine and sine functions, respectively.

The **control problem** can be stated by selecting the design matrices K_p and K_v such as the position error $\tilde{\boldsymbol{q}}$ and the joint velocity $\dot{\boldsymbol{q}}$ vanish asymptotically, i.e., $\lim_{t\to\infty}[\tilde{\boldsymbol{q}}(t),\ \dot{\boldsymbol{q}}(t)]^T = \mathbf{0} \in \mathbb{R}^{2n}$.

Proposition. Consider the robot dynamic model (1), together with the control law (2), then the closed–loop system is globally asymptotically stable and the positioning aim $\lim_{t\to\infty}\boldsymbol{q}(t) = \boldsymbol{q}_d \wedge \lim_{t\to\infty}\dot{\boldsymbol{q}}(t) = \mathbf{0}$ is achieved.

Proof: The closed–loop system equation obtained by combining the robot dynamic model (1) and control scheme (2) can be written as

$$\frac{d}{dt}\begin{bmatrix}\tilde{\boldsymbol{q}}\\ \dot{\boldsymbol{q}}\end{bmatrix} = \begin{bmatrix} -\dot{\boldsymbol{q}} \\ M^{-1}(\boldsymbol{q})\left[K_p\frac{ch(\lambda\tilde{\boldsymbol{q}})^{m-1}sh(\lambda\tilde{\boldsymbol{q}})}{1+ch(\lambda\tilde{\boldsymbol{q}})^{m}} - K_v\frac{ch(\alpha\dot{\boldsymbol{q}})^{m-1}sh(\alpha\dot{\boldsymbol{q}})}{1+ch(\alpha\dot{\boldsymbol{q}})^{m}} - C(\boldsymbol{q},\dot{\boldsymbol{q}})\dot{\boldsymbol{q}}\right] \end{bmatrix} \quad (5)$$

which is an autonomous differential equation. Now, it is demonstrated that the equilibrium point exists and it is unique.

Note that $-\dot{\boldsymbol{q}} = \mathbf{0} \Rightarrow$ -$I\dot{\boldsymbol{q}} = \mathbf{0} \Rightarrow \dot{\boldsymbol{q}} = \mathbf{0}$, where $I \in \mathbb{R}^{n\times n}$ is the identity matrix.

For the second component of the equation (5) $C(\boldsymbol{q},\dot{\boldsymbol{q}}) = 0$ according to the property (3). $M(\boldsymbol{q}) > 0 \Rightarrow \exists\ M(\boldsymbol{q})^{-1} > 0$ therefore

$$\begin{aligned} M(\boldsymbol{q})^{-1}K_p\frac{ch(\lambda\tilde{\boldsymbol{q}})^{m-1}sh(\lambda\tilde{\boldsymbol{q}})}{1+ch(\lambda\tilde{\boldsymbol{q}})^{m}} &= 0 \Leftrightarrow sh(\lambda\tilde{q_i}) = 0 \\ sh(\lambda\tilde{q_i}) &= 0 \Leftrightarrow \tilde{q_i} = 0 \quad (6) \end{aligned}$$

Then

$$K_p\frac{ch(\lambda\tilde{\boldsymbol{q}})^{m-1}sh(\lambda\tilde{q})}{1+ch(\lambda\tilde{q})^{m}} = 0 \Leftrightarrow \tilde{q_i} = 0 \quad (7)$$

with $kp_i \in \Re+$, $K_p = diagonal(k_{pi})$

Therefore the origin of the state space is its unique equilibrium point.

To carry out the stability analysis of equation (5), the following Lyapunov function candidate is proposed:

$$\begin{aligned} V(\tilde{\boldsymbol{q}},\dot{\boldsymbol{q}}) &= \frac{1}{2}\dot{\boldsymbol{q}}^T M(\boldsymbol{q})\dot{\boldsymbol{q}} \\ &+\frac{1}{m}\begin{bmatrix} \sqrt{ln(\frac{1+ch(\lambda\tilde{q_1})^m}{2})} \\ \vdots \\ \sqrt{ln(\frac{1+ch(\lambda\tilde{q_n})^m}{2})} \end{bmatrix}^T \\ &\Lambda^{-1}Kp\begin{bmatrix} \sqrt{ln(\frac{1+ch(\lambda\tilde{q_1})^m}{2})} \\ \vdots \\ \sqrt{ln(\frac{1+ch(\lambda\tilde{q_n})^m}{2})} \end{bmatrix} \quad (8) \end{aligned}$$

where Λ^{-1} is a diagonal matrix and it is represented as:

$$\Lambda = \begin{bmatrix} \frac{1}{\lambda_1} & \cdots & 0 \\ \vdots & \ddots & \vdots \\ 0 & \cdots & \frac{1}{\lambda_n} \end{bmatrix} \quad (9)$$

The first term of $V(\tilde{\boldsymbol{q}},\dot{\boldsymbol{q}})$ is a positive definite function with respect to $\dot{\boldsymbol{q}}$ because $M(\boldsymbol{q})$ is a positive definite matrix. The second term of Lyapunov function candidate (8), which can be interpreted as a potential energy induced by the position error is also a positive definite function with respect to position error $\tilde{\boldsymbol{q}}$, because K_p is a positive definite diagonal matrix.

Therefore, the Lyapunov function candidate (8) is a radially unbounded and globally positive definite function.

The time derivative of Lyapunov function candidate (8) is:

$$\dot{V}(\tilde{\boldsymbol{q}},\dot{\boldsymbol{q}}) = \dot{\boldsymbol{q}}^T M(\boldsymbol{q})\ddot{\boldsymbol{q}} + \frac{1}{2}\dot{\boldsymbol{q}}^T\dot{M}(\boldsymbol{q})\dot{\boldsymbol{q}}$$

$$+\begin{bmatrix} \sqrt{ln(\frac{1+ch(\lambda_1\tilde{q}_1)^m}{2})} \\ \vdots \\ \sqrt{ln(\frac{1+ch(\lambda_n\tilde{q}_n)^m}{2})} \end{bmatrix}^T$$
$$\Lambda^{-1}K_p \begin{bmatrix} \frac{\frac{ch(\lambda\hat{q}_i)^{m-1}sh(\lambda\hat{q}_i)}{1+ch(\lambda\hat{q}_i)^m}}{\sqrt{ln(\frac{1+ch(\lambda\tilde{q}_i)^m}{2})}} \end{bmatrix} \dot{\tilde{\boldsymbol{q}}} \quad (10)$$

along the trajectories of the closed–loop equation (5) is:

$$\begin{aligned} \dot{V}(\tilde{\boldsymbol{q}},\dot{\boldsymbol{q}}) &= \dot{\boldsymbol{q}}^T K_p \frac{ch(\lambda\hat{q}_i)^{m-1}sh(\lambda\hat{q}_i)}{1+ch(\lambda\hat{q}_i)^m} \\ &\quad -\dot{\boldsymbol{q}}^T K_v \frac{ch(\lambda\dot{q}_i)^{m-1}sh(\lambda\dot{q}_i)}{1+ch(\lambda\dot{q}_i)^m} \\ &\quad -\dot{\boldsymbol{q}}^T C(\boldsymbol{q},\dot{\boldsymbol{q}})\dot{\boldsymbol{q}} + \frac{1}{2}\dot{\boldsymbol{q}}^T \dot{M}(\boldsymbol{q})\dot{\boldsymbol{q}} \\ &\quad -\dot{\boldsymbol{q}}^T K_p \frac{ch(\lambda\hat{q}_i)^{m-1}sh(\lambda\hat{q}_i)}{1+ch(\lambda\hat{q}_i)^m} \quad (11) \end{aligned}$$

and after some algebra is:

$$\begin{aligned} \dot{V}(\tilde{\boldsymbol{q}},\dot{\boldsymbol{q}}) &= -\dot{\boldsymbol{q}}^T K_v \frac{ch(\lambda\dot{q}_i)^{m-1}sh(\lambda\dot{q}_i)}{1+ch(\lambda\dot{q}_i)^m} \\ &\quad +\dot{\boldsymbol{q}}^T \left[\frac{1}{2}\dot{M}(\boldsymbol{q}) - C(\boldsymbol{q},\dot{\boldsymbol{q}})\right]\dot{\boldsymbol{q}} \quad (12) \end{aligned}$$

and using the property 2 it can be written as:

$$\dot{V}(\tilde{\boldsymbol{q}},\dot{\boldsymbol{q}}) = -\dot{\boldsymbol{q}}K_v \begin{bmatrix} \frac{ch(\alpha\dot{q}_1)^{m-1}sh(\alpha\dot{q}_1)}{1+ch(\alpha\dot{q}_1)^m} \\ \vdots \\ \frac{ch(\alpha\dot{q}_n)^{m-1}sh(\alpha\dot{q}_n)}{1+ch(\alpha\dot{q}_n)^m} \end{bmatrix} \leq 0 \quad (13)$$

which is a negative semidefinite funtion, therefore we concluded that the equilibrium point is stable. In order to prove the asymptotic stability in a global way, we make use of the autonomous nature of closed-loop (2) when we applied the *LaSalle's invariance principle*:
In the region

$$\Omega = \left\{ \begin{bmatrix} \tilde{\boldsymbol{q}} \\ \dot{\boldsymbol{q}} \end{bmatrix} \in \Re^n : \dot{V}(\tilde{\boldsymbol{q}},\dot{\boldsymbol{q}}) = 0 \right\} \quad (14)$$

the unique invariant is $\left[\tilde{\boldsymbol{q}}^T \ \dot{\boldsymbol{q}}^T\right]^T = 0 \in R^{2n}$, therefore $\lim_{t\to\infty} \begin{bmatrix} \tilde{\boldsymbol{q}}(t) \\ \dot{\boldsymbol{q}}(t) \end{bmatrix} \to 0$.

4 Experimental Set-Up

An experimental system for researching robot control algorithms has been designed and built at The "Benemérita Universidad Autónoma de Puebla". It is a direct–drive robot manipulator with three degrees of freedom moving in 3–dimensional space (see Figure 1).

Figure 1: Experimental robot. Home position

The experimental robot consists of links made of 6061 aluminum, actuated by brushless direct drive servo actuator from Parker Compumotor to drive the joints without gear reduction. Advantages of this type of direct-drive actuator includes freedom from backslash and significantly lower joint friction compared with actuators composed by gear drives. The motors used in the experimental robot are listed in Table 1.

Table 1: Servo actuators of the experimental robot.

Link	Model	Torque [Nm]	p/rev
Base	DM-1015B-60	15	2621440
Shoulder	DM-1050A-115	50	4096000
Elbow	DM-1004C-115	4	2621440

The servos are operated in torque mode, so the motors act as torque source and they accept an analog voltage as a reference of torque signal. Position information is obtained from incremental encoders located on the motors. The standard backwards difference algorithm applied to the joint position measurements was used to generate the velocity signals. The manipulator workspace is a sphere with a radius of 1m.
Besides position sensors and motor drivers, the manipulator also includes a motion control board manufactured by Precision MicroDynamic Inc., which is used to obtain the joint positions. The control algorithm runs on a Pentium–II (333 Mhz) host computer.
With reference to our direct–drive robot, only the gravitational vector is required to implement the new family of controllers (2), which is available in [34]

$$\boldsymbol{g}(\boldsymbol{q}) = \begin{bmatrix} 0 \\ 1.02\,\sin(q_1) + 0.20\,\sin(q_1+q_2) \\ 0.20\,\sin(q_1+q_2) \end{bmatrix} \quad [\text{Nm}]. \tag{15}$$

5 Experimental Results

In this Section an experimental comparison of five position controllers on a three–degrees–of–freedom direct-drive robot manipulator to support our theoretical developments is presented. To investigate the performance among controllers, they have been clasified to them as E2H, E3H and E4H for the exponential hyperbolic family where the exponential m = 2, 3 and 4, respectively. We denote TANH for Hyperbolic Tangent controller and PD for the simple PD controller.
In order to compare the perfomance of the controllers on direct - drive robot, an experiment of position control whose objective is to move the manipulator end - effector from its initial position to a fixed desired target has been designed. For the present application the desired joint positions were chosen as: $[q_{d1}, q_{d2}, q_{d3}]^T = [45, 45, 90]^T$ degrees, where q_{d1}, q_{d2}, q_{d3} represents the base, shoulder, and elbow joints, respectively. The initial positions and velocities were set to zero (for example in home position). The friction phenomenona were not modeled for compensation purpose. As a result, all the controllers did not show any type of friction compensation, therefore it has been decided to consider the friction unmodeled dynamics. Evaluated controllers have been written in C language. The sampling rate was executed at 2.5 msec. Figure 1 and Figure 2 shows the initial and desired configuration for the experimental robot, respectively.

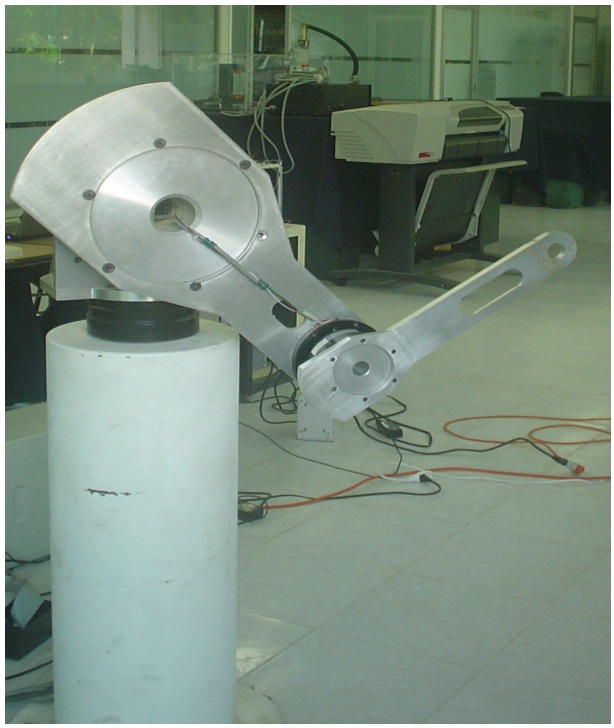

Figure 2: Desired position for experimental robot

5.1 Experimental Results for the Exponencial Hyperbolic family controller

From equation (2), with n = 3 degrees of freedom for the experimental arm, (see Figure 1)the following class of controllers can be obtained:
With the exponential m = 2, this member of the family is called E2H, the equation for the three joints of the robot arm are given as:

$$\begin{aligned} \boldsymbol{\tau}_{E2H_1} &= K_{p1}\frac{ch(\lambda_1\tilde{q_1})sh(\lambda_1\tilde{q_1})}{1+ch(\lambda_1\tilde{q_1})^2} \\ &\quad -K_{v1}\frac{ch(\alpha\dot{q_1})sh(\alpha\dot{q_1})}{1+ch(\alpha\dot{q_1})^2} \\ \boldsymbol{\tau}_{E2H_2} &= K_{p2}\frac{ch(\lambda_2\tilde{q_2})sh(\lambda_2\tilde{q_2})}{1+ch(\lambda_2\tilde{q_2})^2} \\ &\quad -K_{v2}\frac{ch(\alpha\dot{q_2})sh(\alpha\dot{q_2})}{1+ch(\alpha\dot{q_2})^2} \end{aligned}$$

$$
\begin{aligned}
& +1.02\sin(q_2)+0.2\sin(q_2+q_3) \\
\boldsymbol{\tau}_{E2H_3} &= K_{p3}\frac{ch(\lambda_3\tilde{q_3})sh(\lambda_3\tilde{q_3})}{1+ch(\lambda_3\tilde{q_3})^2} \\
& -K_{v3}\frac{ch(\alpha\dot{q_3})sh(\alpha\dot{q_3})}{1+ch(\alpha\dot{q_3})^2} \\
& +0.2\sin(q_2+q_3) \qquad (16)
\end{aligned}
$$

With the exponential m = 3, this member of the family is called E3H, the equation for the three joints of the robot arm are given as:

$$
\begin{aligned}
\boldsymbol{\tau}_{E3H_1} &= K_{p1}\frac{ch(\lambda_1\tilde{q_1})^2sh(\lambda_1\tilde{q_1})}{1+ch(\lambda_1\tilde{q_1})^3} \\
& -K_{v1}\frac{ch(\alpha\dot{q_1})^2sh(\alpha\dot{q_1})}{1+ch(\alpha\dot{q_1})^3} \\
\boldsymbol{\tau}_{E3H_2} &= K_{p2}\frac{ch(\lambda_2\tilde{q_2})^2sh(\lambda_2\tilde{q_2})}{1+ch(\lambda_2\tilde{q_2})^3} \\
& -K_{v2}\frac{ch(\alpha\dot{q_2})^2sh(\alpha\dot{q_2})}{1+ch(\alpha\dot{q_2})^3} \\
& +1.02\sin(q_2)+0.2\sin(q_2+q_3) \\
\boldsymbol{\tau}_{E3H_3} &= K_{p3}\frac{ch(\lambda_3\tilde{q_3})^2sh(\lambda_3\tilde{q_3})}{1+ch(\lambda_3\tilde{q_3})^3} \\
& -K_{v3}\frac{ch(\alpha\dot{q_3})^2sh(\alpha\dot{q_3})}{1+ch(\alpha\dot{q_3})^3} \\
& +0.2\sin(q_2+q_3) \qquad (17)
\end{aligned}
$$

With the exponential m = 4, this member of the family is called E4H, the equation for the three joints of the robot arm are given as:

$$
\begin{aligned}
\boldsymbol{\tau}_{E4H_1} &= K_{p1}\frac{ch(\lambda_1\tilde{q_1})^3sh(\lambda_1\tilde{q_1})}{1+ch(\lambda_1\tilde{q_1})^4} \\
& -K_{v1}\frac{ch(\alpha\dot{q_1})^3sh(\alpha\dot{q_1})}{1+ch(\alpha\dot{q_1})^4} \\
\boldsymbol{\tau}_{E4H_2} &= K_{p2}\frac{ch(\lambda_2\tilde{q_2})^3sh(\lambda_2\tilde{q_2})}{1+ch(\lambda_2\tilde{q_2})^4} \\
& -K_{v2}\frac{ch(\alpha\dot{q_2})^3sh(\alpha\dot{q_2})}{1+ch(\alpha\dot{q_2})^4} \\
& +1.02\sin(q_2)+0.2\sin(q_2+q_3) \\
\boldsymbol{\tau}_{E4H_3} &= K_{p3}\frac{ch(\lambda_3\tilde{q_3})^3sh(\lambda_3\tilde{q_3})}{1+ch(\lambda_3\tilde{q_3})^4} \\
& -K_{v3}\frac{ch(\alpha\dot{q_3})^3sh(\alpha\dot{q_3})}{1+ch(\alpha\dot{q_3})^4} \\
& +0.2\sin(q_2+q_3) \qquad (18)
\end{aligned}
$$

where ($\tau_{E2H_1}, \tau_{E3H_1}$, and τ_{E4H_1}), ($\tau_{E2H_2}, \tau_{E3H_2}$, and τ_{E4H_2}), ($\tau_{E2H_3}, \tau_{E3H_3}$, and τ_{E4H_3}) represent the applied torques for the base, shoulder, and elbow joints, respectively.

The controllers gains were selected empirically. However, several trials for selecting gains were necessary in order to ensure an acceptable behavior in practice, this is, fast response and smaller steady - state error.

In order to avoid torque saturation of the actuators, but works in its linear part, the proportional gains were chosen such that $\tau < \|\tau_{max}\|$, where τ_{max} represents the maximum applied torque of the $\imath$th joint (see limits of actuators in Table 1).

The empirical formula that was used to select the tuning of the proportional gain is given by: $kp_i = 80\%\tau_{imax}/q_{di}$.

In order to decrease the error, λ factor needs to be increased. While λ increases, the slope of the scheme also increases, for that reason the maximum value is applied for lower errors. With the proportional gains fixed, derivative ones were adjusted to obtain a low under - damped response. For a lower α is obtained a proportional relation between velocity and derivative value.

The K_p and K_v matrixes for this proposed family of controllers are the same for E2H, E3H, E4H, that corresponds to the exponent, m = 2, 3 and 4. Values for k_{pi} , k_{vi} and λ_i , α are shown in Table 2 and 3, respectively

Table 2: Settings for Exponent Hyperbolic, k_{pi} and k_{vi} values.

k_p	[Nm]	k_v	[Nm]
k_{p1}	12	k_{v1}	60
k_{p2}	32	k_{v2}	8
k_{p3}	3.2	k_{v3}	0.5

Table 3: Settings for Exponent Hyperbolic, λ_i and α values.

λ	$[\frac{rad}{degrees}]$	α	$[\frac{rad*s}{degrees}]$
λ_1	$\frac{3.14}{4}$	α	$\frac{3.14}{1000}$
λ_2	$\frac{3.14}{0.75}$		
λ_3	$\frac{3.14}{1.4}$		

Figures 3 to 8 contain the experimental results of the exponential hyperbolic family. There are three members of the family E2H, E3H, E4H, for

each one are the graphic of position error and applied torque. The graphics of position error show that the three links tend to a small neighborhood near zero. This characteristic demonstrates the properties of this proposed family. The graphic of applied torque shows that the actuator works in its linear zone but not in the saturation one.

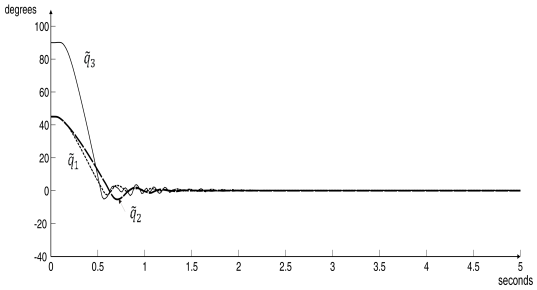

Figure 3: Position errors of the E2H controller.

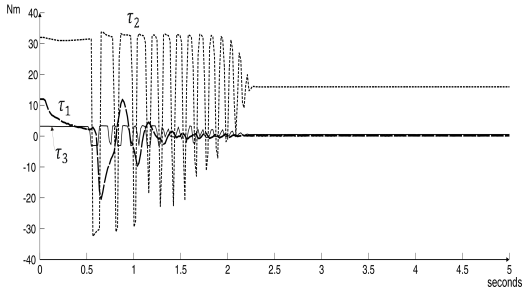

Figure 4: Applied torques of the E2H controller.

Figures 3 and 4, correspond to the E2H controller. The steady state position begins approximately at t = 2 sec, and $[\tilde{q}_1, \tilde{q}_2, \tilde{q}_3]^T = [0.0258, 0.1804, 0.1038]^T$ degrees.

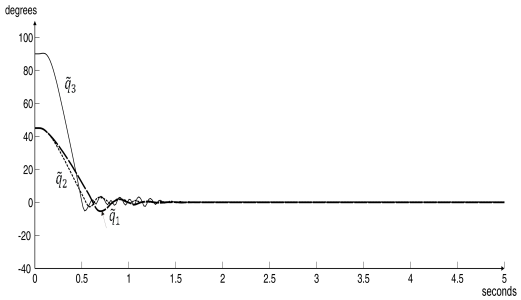

Figure 5: Position errors of the E3H controller.

Figures 5 and 6, correspond to the E3H controller . The steady state position approximately begins at t = 1.5 sec., and $[\tilde{q}_1, \tilde{q}_2, \tilde{q}_3]^T = [0.0110, 0.1804, 0.100]^T$ degrees.

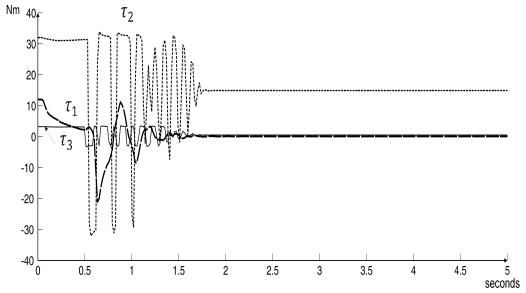

Figure 6: Applied torques of the E3H controller.

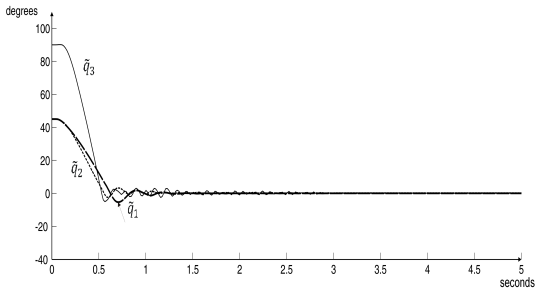

Figure 7: Position errors of the E4H controller.

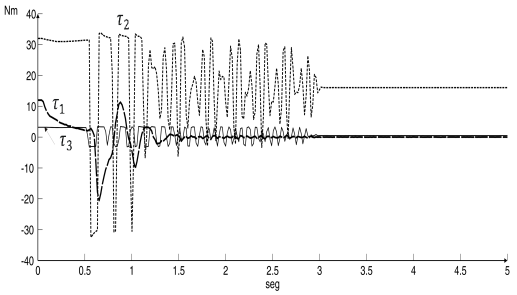

Figure 8: Applied torques of the E4H controller.

Figures 7 and 8, correspond to the E4H controller. The steady state position begins at t = 3 sec., and $[\tilde{q}_1, \tilde{q}_2, \tilde{q}_3]^T = [0.0027, 0.1811, 0.1027]^T$ degrees.

5.2 Experimental Results for the Hyperbolic Tangent and PD controllers

This Section presents the results of the Hyperbolic Tangent and PD controllers, the desired position and initial conditions were the same as in previous Section. Figures 9 to 12 contain the experimental results of this part. The TANH and

PD controllers for the three degrees of freedom robot arm are given by the following equations.

$$\begin{aligned}\boldsymbol{\tau}_{TANH_1} &= K_{p1}\tanh(\tilde{q_1}) - K_{v1}\tanh(\dot{q_1}) \\ \boldsymbol{\tau}_{TANH_2} &= K_{p2}\tanh(\tilde{q_2}) - K_{v2}\tanh(\dot{q_2}) \\ &\quad +1.02\sin(q_2) + 0.2\sin(q_2+q_3) \\ \boldsymbol{\tau}_{TANH_3} &= K_{p3}\tanh(\tilde{q_3}) - K_{v3}\tanh(\dot{q_3}) \\ &\quad +0.2\sin(q_2+q_3) \qquad (19)\end{aligned}$$

$$\begin{aligned}\boldsymbol{\tau}_{PD_1} &= K_{p1}(\tilde{q_1}) - K_{v1}(\dot{q_1}) \\ \boldsymbol{\tau}_{PD_2} &= K_{p2}(\tilde{q_2}) - K_{v2}(\dot{q_2}) \\ &\quad +1.02\sin(q_2) + 0.2\sin(q_2+q_3) \\ \boldsymbol{\tau}_{PD_3} &= K_{p3}(\tilde{q_3}) - K_{v3}(\dot{q_3}) \\ &\quad +0.2\sin(q_2+q_3) \qquad (20)\end{aligned}$$

where $(\tau_{TANH_1}, \tau_{PD_1})$, $(\tau_{TANH_2}, \tau_{PD_2})$, $(\tau_{TANH_3}, \tau_{PD_3})$ represent the applied torques for the base, shoulder, and elbow joints, respectively. Extensive experiments were carried out with the TANH and PD controllers to select their gains, such that the best time response without overshoot and minimum steady - state position error were obtained without going into the saturation zone of the actuator's torques. The TANH and PD gains were selected as: $kp_i = 80\% \mid \boldsymbol{\tau}_{i_{max}} \mid /\tilde{q}_i(0)$ and $k_{vi} << k_{pi}$. After a trial and error procedure, proportional and derivative gains have been selected as suitable choices for preventing the actuators from saturing. Values for k_{pi} and k_{vi} for TANH and PD controllers are shown in Table 3 and 4, respectively.

Table 4: Settings for Hyperbolic Tangent controller.

k_p	[Nm]	k_v	[Nm]
k_{p1}	4	k_{v1}	1.6
k_{p2}	32	k_{v2}	4
k_{p3}	3.2	k_{v3}	0.4

Table 5: Settings for PD controller.

k_p	[Nm]	k_v	[Nm]
k_{p1}	0.3	k_{v1}	6E-4
k_{p2}	0.9	k_{v2}	1E-2
k_{p3}	0.045	k_{v3}	1E-3

Figure 9 contains the experimental results of position errors of Hyperbolic Tangent controller. The steady state position begins approximately between t = 1.5 and 2 sec. and $[\tilde{q_1}, \tilde{q_2}, \tilde{q_3}]^T = [0.0698, 0.5266, 0.1379]^T$degrees

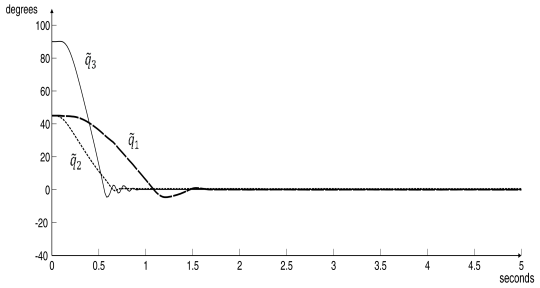

Figure 9: Position errors for the Hyperbolic Tangent controller.

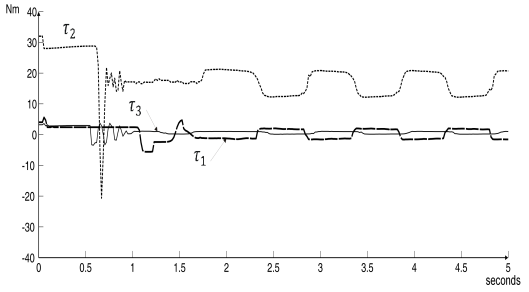

Figure 10: Applied torques of the Hyperbolic Tangent controller.

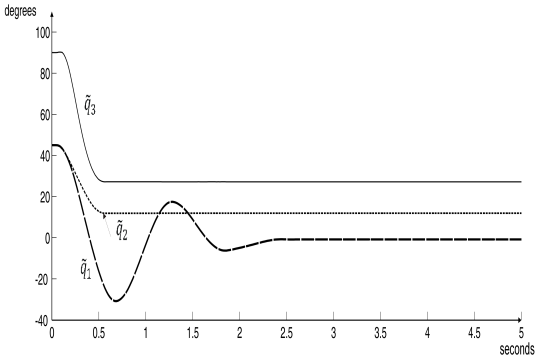

Figure 11: Position errors of the PD controller.

Figures 10 and 12 show the applied torque with Hyperbolic Tangent and PD controller for the base, shoulder and elbow. These curves are inside the limits of torque of its respective actuator but not in the saturation zone. Figure 11 contains the experimental result of position errors of PD controller. The steady state position begins approximately at t = 2.5 sec., and

$[\tilde{q}_1, \tilde{q}_2, \tilde{q}_3]^T = [0.8108, 11.9658, 27.1879]^T$ degrees.

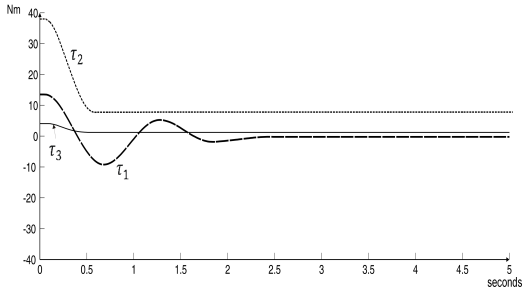

Figure 12: Applied torques of the PD controller.

5.3 Indices of Performance

The robot manipulators are very complex mechanical systems, due to the nonlinear and multivariable nature of their dynamical behavior. For this reason, in the robotic community there are no well–established criteria for proper evaluation of controllers for robots. However, it is accepted in practice to compare the performance of controllers by using the scalar–valued $\mathcal{L}^2$ norm as an objective numerical measure for an entire error curve Whitcomb et. al [24] De Jager & Banens [36] Berghuis et. al [37] Jaritz & Spong [38] The $\mathcal{L}^2[\tilde{\boldsymbol{q}}]$ norm measures the root–mean–square average of the $\tilde{\boldsymbol{q}}$ position error, which is given by:

$$\mathcal{L}^2[\tilde{\boldsymbol{q}}] = \sqrt{\frac{1}{t-t_0}\int_{t_0}^{t} \|\tilde{\boldsymbol{q}}\|^2 dt} \qquad (21)$$

where $t_0, t \in \mathbb{R}_+$ are the initial and final times, respectively. A smaller $\mathcal{L}^2[\tilde{\boldsymbol{q}}]$ represents smaller position error and it is the best performance of the evaluated controller. The data are compared with respect to Hyperbolic Tangent and PD controller. The average of $\mathcal{L}^2$ norm for the several test are the following: 26.22, 26.13, 26.00, 28.25, 37.94 degrees for E2H, E3H, E4H, TANH and PD respectively.

The overall results are summarized by Figure 13 which includes the performance indices of all the controllers. To average out stochastic influences, the data presentation in this Figure represents the mean of root - mean - square position error vector norm of ten runs. In general the proposed controller improves the perfomance of Hyperbolic Tangent and PD in approximately 7.5 % and 31 % respectively. The perfomance of the three members of the proposed family (E2H, E3H, E4H) are almost the same.

The result from one run to another was observed, and the difference with the average are the following: 0.5%, 0.7 %, 0.1%, 0.11 %, 0.43% for E2H, E3H, E4H, TANH and PD respectively, which underscore the repeatability of the experiments.

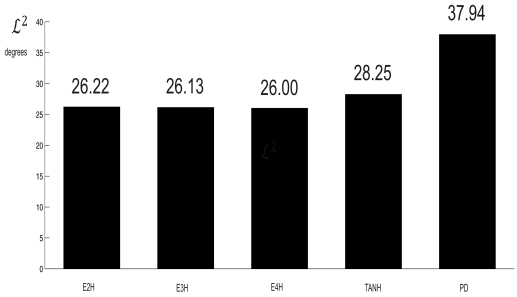

Figure 13: Performance index for transient and stationary states.

In order to compare the error, the values of $\mathcal{L}^2$ norm for stationary state have been obtained (Figure 14) This values are taken in the last second of each test, between the 4th and 5th second, and are the following: 0.07, 0.07, 0.07, 0.2 and 10.41 degrees for E2H, E3H, E4H, TANH and PD, respectively.

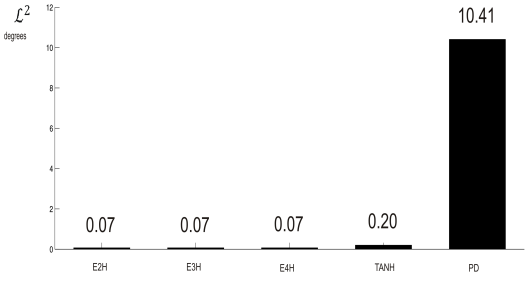

Figure 14: Performance index for stationary state case.

Figure 14 shows the results and evidence for the poor perfomance of the PD controller in the stationary state.

The $\mathcal{L}^2$ norm for stationary state of the proposed controller is 0.13 degrees less than Hyperbolic Tangent that represents the 65 %. With respect to the PD controller is 10.34 degrees.

6 Conclusions

In this paper a new scheme for position control of robot manipulator has been introduced, that is, the exponential hyperbolic family of controllers. It is supported by a rigorous stability analysis and the theoretical results establish conditions for ensuring global regulation.

The performance of the new scheme was compared with other algorithms such as Hyperbolic Tangent and PD controllers by using a time - real experimental comparison on a three degrees of freedom direct - drive robot. From experimental results the new scheme was sufficient to produce a brief transient and minimum steady - state position error in comparison with Hyperbolic Tangent and PD controllers that showed to be less robust than the proposed scheme.

This new family show the less $\mathcal{L}^2[\tilde{q}]$ norm, therefore the best performance among evaluated controllers and the less $\mathcal{L}^2[\tilde{q}]$ norm for stationary state, that indicate the minimum error among evaluated controllers. For this reason, the usefulness of the proposed family can be concluded to represent an attractive scheme from a practical viewpoint for example in manufacturing systems.

References:

1. Y. Su, D. Sun, L. Ren, and J. K. Mills, Integration of Saturated PI Synchronous Control and PD Feedback for control of parallel manipulators. *IEEE Transactions on Robotics.* Vol. 22, No.1, 2006, pp.202-207.

2. M. Sun, S. S. Ge, and I. M. Y. Mareels. Adaptive Repetitive Learning Control of Robotic Manipulators Without The Requirement for Initial Repositioning. *IEEE Transactions on Robotics.* Vol. 22, No.3, 2006, pp.563-568.

3. E. Jarzebowska . Control oriented dynamic formulation for robotic systems with program constraints. *Robotica, Cambridge University Press* Vol.24, 2006, pp.61-73.

4. V. Santibañez, R. Kelly. and M. Llama. A novel global asymptotic stable set-point fuzzy controller with bounded torques for robot manipulators.*IEEE Transactions on Fuzzy Systems.* Vol. 13, No.3, 2005, pp.362-372.

5. R. Kelly, A tuning procedure for stable PID control of robot manipulators. *Robotica, Cambridge University Press*, Vol. 13, 1995, pp.141-148.

6. L. Sciavicco, & B. Siciliano, *Modeling and Control of Robot Manipulators* The McGraw–Hill Companies, Inc. 1996.

7. C. Canudas, B. Siciliano, & G. Bastin, *Theory of Robot Control.* Springer, 1996.

8. B. Paden, & R. Panja, Globally asymptotically stable PD+ controller for robot manipulator.*International Journal of Control*, Vol.47, No.6, 1988, pp.1697-1712.

9. H. K. Khalil, *Nonlinear Systems.* Prentice–Hall, 2002.

10. M. Takegaki, & S. Arimoto, A new feedback method for dynamic control of manipulators. *J. Dyn. Syst. Meas. Control Transactions. ASME* Vol. 103, 1981, pp.119-125.

11. S. Arimoto, and F. Miyazaki, *Stability and robustness of PD feedback control with gravity compensation for robot manipulator.* Robotics: Theory and Application - DSC, F. W. Paul and D. Youcef-Toumi Eds. Vol.3, 1986, pp. 67-72.

12. R. Kelly, Regulation of manipulators in generic task space: An energy shaping plus damping injection approach.*IEEE Transactions on Robotics and Automation.* Vol 15, No.2, 1999, pp.381–386.

13. R. Kelly, & R. Carelli, A class of nonlinear PD–Type controllers for robot manipulators. *Journal of Robotic Systems.* Vol.13, No.12, 1996, pp.793–802.

14. H. Seraji A new class of nonlinear PID controllers with robotic applications. *Journal of Robotic Systems.* Vol. 15, No.3, 1998, pp.61-81.

15. T. C. Hsia, Robustness analysis of a PD controller with approximate gravity compensation for robot manipulator control. *Journal of Robotic System.* Vol. 11, No.6, 1994, pp.517-521.

16. V. Santibaez, R. Kelly, & F. Reyes, A new set–point controller with bounded torques for robot manipulators. *IEEE Transactions on Industrial Electronics.* Vol.45, No.1, 1998, pp.126–133.

17. A. Loria, E. Lefeber, & H. Nijmeijer, Global asymptotic stability of robot manipulators with linear PID and PI^{2}D control. *Journal on Stability and Control: Theory and Applications SACTA*, Vol.3, No,2. 2000, pp.138–148.

18. F. Reyes, and A. Rosado, Polynomial family of PD-Type controllers for robot manipulators. *Control Engineering Practice, Elsevier Ed.* Vol.13, 2005, 2005, pp. 441-450.

19. D. Koditschek, Natural motion for robot arms. *Proceedings of the 1984 IEEE Conference on Decision and Control.* Las Vegas N, 1984, pp.733–735.

20. D. Koditschek, Strict global Lyapunov function for mechanical systems. *Proceedings of the IEEE American Control Conference.* Atlanta GA. 1988, pp.1770-1775.

21. J. T. Wen, A unified perspective on robot control: the energy Lyapunov function approach. *International Journal Adaptive Control Signal Proceedings.* No 4, 1990, pp.487-500.

22. J. T. Wen, K. Delgado and D. Bayard. Lyapunov function-based control laws for revolute robot arms: tracking control, robustness, and adaptive control. *IEEE transactions on Automatic Control*, AC-37, 1992, pp.231-237.

23. P. Tomei, Adaptive PD Controller for robot manipulators, *IEEE Transactions on Robotics and Automation*, RA-7, 1991, pp.564-570.

24. L. L. Whitcomb, A. A. Rizzi, & D. E. Koditschek, Comparative experiments with a new adaptive controller for robot arms, *IEEE Transactions on Robotics and Automation*, Vol. 9, No. 1, 1993, pp.59–69.

25. V. Santibaez, R. Kelly. Strict Lyapunov Functions for control of robot manipulators. *Automatica*, Vol. 33. No. 4, 1997, pp.675-682.

26. T. Hu, and Z. Lin, Composite Quadratic Lyapunov functions for constrained control systems.*IEEE Transactions on Automatic Control*, Vol. 48, No.3, 2003, pp.440-450.

27. F. Mazenc, and D. Nesic. Strong Lyapunov functions for systems satisfying the conditions of LaSalle. *IEEE Transactions on Automatic Control* Vol. 49, No.6, 2004, pp.1026-1030.

28. J. Adamy, Implicit Lyapunov functions and isochrones of linear systems. *IEEE Transactions on Automatic Control*, Vol.50, No. 6, 2005, pp. 874-879.

29. S. G. Nersesov, and W. M. Haddad, On the stability and control of nonlinear dynamical systems via Vector Lyapunov Functions. *IEEE Transactions on Automatic Control.* Vol. 51, No.2, 2006, pp.203-215.

30. F. Mazenc and M Malisoff, Further constructions of Control-Lyapunov Functions and Stabilizing Feedbacks for Systems Satisfying the Jurdjevic-Quinn Conditions. *IEEE Transactions on Automatic Control.* Vol. 51, No.2, 2006, pp. 360-365.

31. M. W. Spong, & M. Vidyasagar, *Robot Dynamics and Control.* John Wiley and Sons, 1989. 1989).

32. B. Armstrong–Hoélouvry, *Control of Machines with Friction.* Kluwer Academic Publishers 1991.

33. R. Ortega, and M. Spong, Adaptive Motion Control of Rigid Robots: a Tutorial. *Automatica*, Vol.25, No.6, 1989, pp.877–888.

34. F. Reyes, & R. Kelly, Experimental evaluation of identification schemes on a direct drive robot. *Robotica*, Cambridge University Press. Vol.15, 1997, pp.563–571.

35. J. Alvarez, R. Kelly, & I. Cervantes Semiglobal stability of saturated linear PID control for robot manipulators. *Automatica*, Vol. 39, No.6, 2003, pp. 989–995.

36. B. De Jager, & J. Banens, Experimental evaluations of robot controllers. *Proceedings of the 33rd. Conference on Decision and Control.* Lake Buena Vista, Fl. U.S.A., 1994, pp.363–368.

37. H. Berghuis, H. Roebbers & H. Nijmeijer, Experimental comparison of parameter estimation methods in adaptive robot control, *Automatica*, Vol. 31, No. 9, 1995, pp.1275–1285.

38. A. Jaritz & M. Spong.(1996). An experimental comparison of robust control algorithms on a direct drive manipulator. *IEEE Transactions on Control Systems Technology.* Vol.4, No.6, 1996, pp.363–368.

39. W. Wang , S. Lu & C. Hsu, Experiments on the position control of a one - link flexible robot arm. *IEEE Transactions on Robotics and Automation.* Vol.5, No.3, 2002, pp.373 - 377.

40. H. Arai & S. Tachi, Position control of manipulator with passive joints using dynamic coupling. *IEEE Transactions on Robotic and Automation.* Vol. 7, No. 4, 2002, pp.528 – 534.

41. M. Ho & Y. Tu, Position control of a single - link flexible manipulator using H∞ - based PID control. *IEEE Transactions Control Theory and Applications.* Vol. 153, No.5, 2006, pp.615 –622.